

# SEM characterization of sol-gel-derived precursors, novel black pigments and glazes

**Aurelija Gatelytė,**

**Jūratė Senvaitienė,**

**Darius Jasaitis,**

**Aldona Beganskienė,**

**Aivaras Kareiva\***

*Department of General and  
Inorganic Chemistry,  
Vilnius University,  
Naugarduko 24,  
LT-03225 Vilnius,  
Lithuania*

In the present work, the nanosized yttrium iron garnet ( $Y_3Fe_5O_{12}$ ), yttrium perovskite ferrite ( $YFeO_3$ ), cobalt, nickel and zinc iron spinel ( $CoFe_2O_4$ ,  $NiFe_2O_4$  and  $ZnFe_2O_4$ , respectively) powders were synthesized by an aqueous sol-gel process. These compounds have been used for the first time as precursors for the preparation of black ceramic pigments. The possible application of the obtained black ceramic pigments as ceramic glazes was also demonstrated. The microstructural evolution and morphological features of the obtained transition metal ferrites, pigments and glazes were studied by scanning electron microscopy (SEM).

**Key words:** transition metal ferrites, sol-gel process, black ceramic pigments, glazes, SEM

## INTRODUCTION

Iron-containing transition metal oxides possess unique magnetic, magneto-optical, magnetoresistive, thermal, electric and mechanical properties such as ferrimagnetism, excellent creep and radiation damage resistance, high thermal conductivity, high electrical resistivity, controllable saturation magnetization, moderate thermal expansion coefficients, energy-transfer efficiency, narrow linewidth in ferromagnetic resonance and others [1–9]. These properties make iron-containing oxides suitable for numerous device applications. Since these magneto-particles have also been shown to be non-cytotoxic, they would be suitable for also biotechnological applications.

The preparation and characterization of nanosized structures have attracted increasing attention of researchers in the last decade. Moreover, all the mentioned properties of iron-containing oxide ceramics are highly sensitive not only to changes in dopant composition or host stoichiometry, but also to the processing conditions, which are very much responsible for the crystallinity, crystal shape, crystal size, crystal size distribution and phase purity of the resulting powders.

To prepare these iron-containing mixed oxides, the oxide-mixing method, based on the solid state reaction between the component metal oxides, is still utilized because of its lower manufacturing cost and simpler preparation process [9–11]. However, this method, in general, requires the calcining temperature higher than 1 000 °C to eliminate the unreacted starting oxides and to obtain the final product of a single phase. In order to overcome these inevitable disadvantages arising from the solid state reaction, some methods including sol-gel, hydrothermal, combustion, spray-pyrolysis, auto-combustion, polymeric precursor route, solvothermal, co-precipitation and redox reaction techniques can be used [8, 12–18].

Over the last few decades, the sol-gel techniques have been used to prepare a variety of mixed-metal oxides, nanomaterials and nanoscale architectures, nanoporous oxides, organic-inorganic hybrids [19–22]. The sol-gel process has been demonstrated to offer considerable advantages such as a better mixing of starting materials and an excellent chemical homogeneity in the final product. Moreover, the molecular level mixing and the tendency of partially hydrolyzed species to form extended networks facilitate the structure evolution thereby lowering the crystallization temperature. In this paper, we present results of the synthesis of nanosized selected transition metal fer-

\* Corresponding author. E-mail: aivaras.kareiva@chf.vu.lt

rites (yttrium iron garnet ( $Y_3Fe_5O_{12}$ ), yttrium perovskite ferrite ( $YFeO_3$ ), cobalt, nickel and zinc iron spinel ( $CoFe_2O_4$ ,  $NiFe_2O_4$  and  $ZnFe_2O_4$ , respectively) powders). Also, in this work we have investigated a possible application of nanoscaled transition metal ferrites synthesized by the sol-gel method as ceramic black pigments and glazes. The results of characterization of the obtained compounds and compositions by scanning electron microscopy (SEM) are presented herein.

## EXPERIMENTAL

Transition metal ferrite ceramic samples ( $YFeO_3$ ,  $Y_3Fe_5O_{12}$ ,  $CoFe_2O_4$ ,  $NiFe_2O_4$ ,  $ZnFe_2O_4$ ) were synthesized by the aqueous glycolate sol-gel method. The gels were prepared using stoichiometric amounts of analytical-grade iron nitrate nonahydrate  $Fe(NO_3)_3 \cdot 9H_2O$ , yttrium oxide  $Y_2O_3$ , cobalt acetate tetrahydrate  $Co(CH_3COO)_2 \cdot 4H_2O$ , nickel acetate tetrahydrate  $Ni(CH_3COO)_2 \cdot 4H_2O$ , and zinc acetate dihydrate  $Zn(CH_3COO)_2 \cdot 2H_2O$  as  $Fe^{3+}$ ,  $Y^{3+}$ ,  $Co^{2+}$ ,  $Ni^{2+}$  and  $Zn^{2+}$  raw materials, respectively. For the preparation of all samples by the sol-gel process, iron nitrate was first dissolved in 50 mL of 0.2 mol/L  $CH_3COOH$  at 65 °C. To this solution, yttrium oxide dissolved in acetic acid, or cobalt acetate, or nickel acetate, or zinc acetate dissolved in 50 mL of distilled water was added, and the resulting mixture was stirred for 1 h at the same temperature. In the following step, 1,2-ethanediol (2 mL) as a complexing agent was added to the reaction solution. After concentrating the solutions by rapid evaporation at 95 °C under stirring, the Y-Fe-O, Co-Fe-O, Ni-Fe-O or Zn-Fe-O nitrate-acetate-glycolate sols turned into brownish transparent gels. The oven-dried (110 °C) precursor gel powders were ground in an agate mortar and preheated for 2 h at 800 °C in the air. After grinding in an agate mortar, the powders were additionally sintered in the air for 10 h at 1 000 °C without any intermediate grinding.

For the preparation of black pigments, the obtained ferrites were mixed with  $CuO$ ,  $Pb_3O_4$  and  $SiO_2$ . The molar ratio of ferrite,  $Pb_3O_4$  and  $SiO_2$  was constant (see Table) in all systems. However, the amount of  $CuO$  was slightly different depending on the colour intensity of a black pigment. These pigments were placed on oven-dried ceramic plates and annealed for 5 h at 800 °C. After heat treatment, black glazes were obtained.

The morphology of the resultant transition metal ferrite powders, pigments and glazes was examined with CamScan or FE-SEM Zeiss Ultra 55 field emission scanning electron microscopes.

## RESULTS AND DISCUSSION

Figure 1 shows the SEM micrograph of  $YFeO_3$  ceramics. The scanning electron micrograph indicates the formation of nanosized crystallites ~200 nm in width and ~1 000 nm in length. The crystallites are necked to each other, forming highly symmetric ornaments. A scanning electron micrograph of sol-gel-derived  $Y_3Fe_5O_{12}$  ceramics synthesized for 10 h at 1 000 °C is shown in Fig. 2. For yttrium aluminium garnet, a similar microstructure was observed as well. Similar, necked to each other crystallites of approximately the same size were formed. However,  $Y_3Fe_5O_{12}$  particles showed a very well pronounced agglomeration, indicating a good connectivity among the grains.

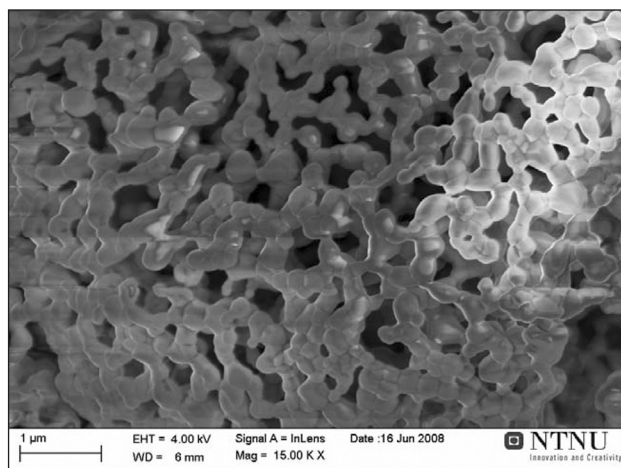


Fig. 1. SEM micrograph of sol-gel-derived  $YFeO_3$  ceramics

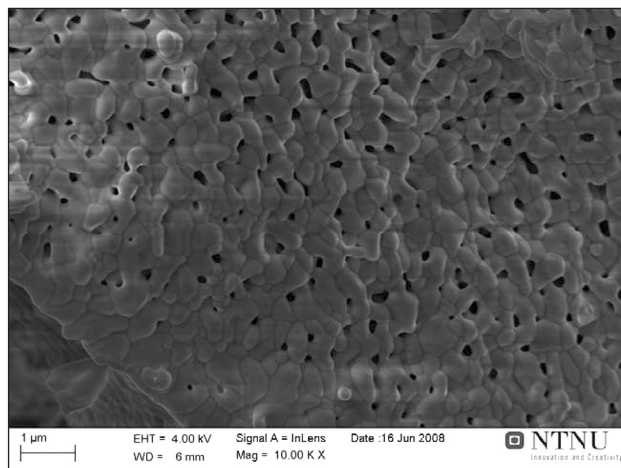


Fig. 2. SEM micrograph of sol-gel-derived  $Y_3Fe_5O_{12}$  ceramics

Table. The chemical composition of black ceramic pigments

| No. | Composition, mol %   |
|-----|--|
| 1   | $Pb_3O_4 : SiO_2 : YFeO_3 : CuO = 0.00146 : 0.000973 : 0.000128 : 0.000256$        |
| 2   | $Pb_3O_4 : SiO_2 : Y_3Fe_5O_{12} : CuO = 0.00146 : 0.000973 : 0.000128 : 0.000128$ |
| 3   | $Pb_3O_4 : SiO_2 : CoFe_2O_4 : CuO = 0.00146 : 0.000973 : 0.000128 : 0.000256$     |
| 4   | $Pb_3O_4 : SiO_2 : NiFe_2O_4 : CuO = 0.00146 : 0.000973 : 0.000128 : 0.000064$     |
| 5   | $Pb_3O_4 : SiO_2 : ZnFe_2O_4 : CuO = 0.00146 : 0.000973 : 0.000128 : 0.000384$     |

Interestingly, almost identical surface microstructure was observed for all spinel crystal structure ceramic samples. Figure 3 shows a SEM micrograph of  $\text{CoFe}_2\text{O}_4$  spinel obtained at 1 000 °C. The SEM micrograph suggests that the  $\text{CoFe}_2\text{O}_4$  solids synthesized by sol-gel route are composed of spherical submicron grains (less than 1000 nm). The spherical particles are formed also in the case of nickel ferrite  $\text{NiFe}_2\text{O}_4$  (see Fig. 4). However, the particle size of spinel ferrites seems to depend on the nature of a transition metal.  $\text{NiFe}_2\text{O}_4$  crystallites were mostly composed of nanoparticles with a size between 100 and 150 nm. A SEM micrograph of  $\text{ZnFe}_2\text{O}_4$  ceramics is presented in Fig. 5. Zinc iron spinel ceramics was formed with an average grain size of less than 500 nm and more than 200 nm. Thus, once again we can conclude that the particle size of spinels depends on the nature of a transition metal ( $\text{CoFe}_2\text{O}_4 > \text{ZnFe}_2\text{O}_4 > \text{NiFe}_2\text{O}_4$ ). Moreover, all three spinels had a mesoporous structure.

The SEM images of novel black ceramic pigments are shown in Figs. 6–10. As is seen from SEM micrographs, the main morphological features of all specimens are very similar and independent on the nature of a transition metal

ferrite. This is not surprising, since the main component in the composition of a pigment is  $\text{Pb}_3\text{O}_4$  (see Table). All five pigments are mostly composed of plate-like crystallites of different size. However, these plate-like crystals are also

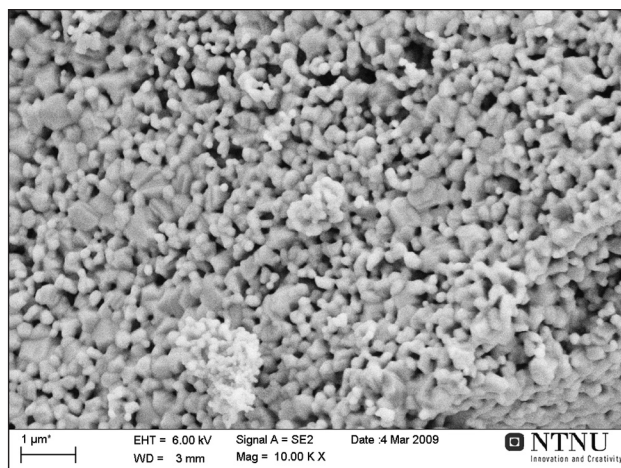


Fig. 5. SEM micrograph of sol-gel-derived  $\text{ZnFe}_2\text{O}_4$  ceramics

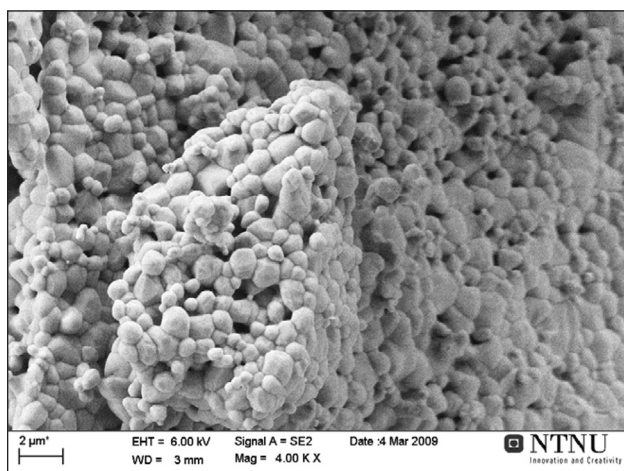


Fig. 3. SEM micrograph of sol-gel-derived  $\text{CoFe}_2\text{O}_4$  ceramics

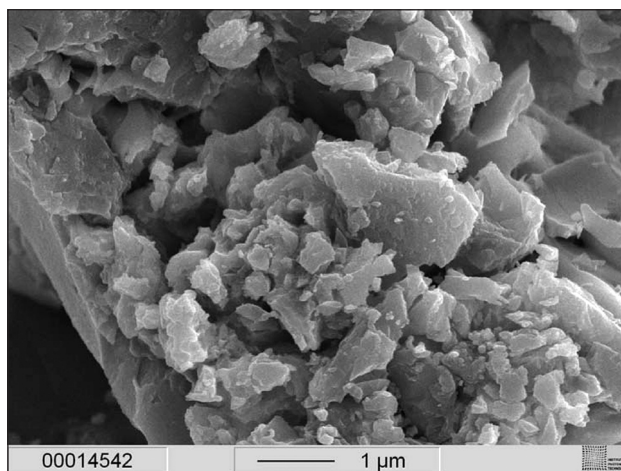


Fig. 6. SEM micrograph of  $\text{YFeO}_3$ -based black pigment

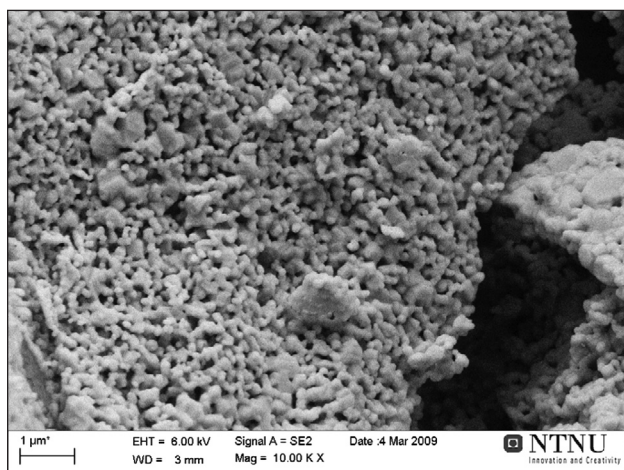


Fig. 4. SEM micrograph of sol-gel-derived  $\text{NiFe}_2\text{O}_4$  ceramics

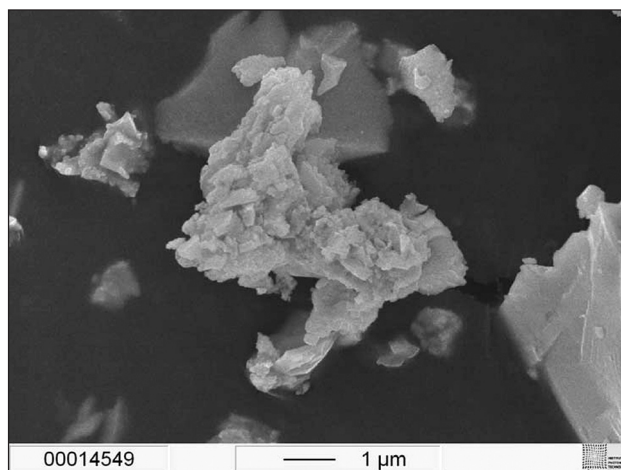


Fig. 7. SEM micrograph of  $\text{Y}_3\text{Fe}_5\text{O}_{12}$ -based black pigment

covered with smaller differently shaped (spherical, needle-like, sticks) particles. The particle size changes in the range of 100 nm to 3  $\mu\text{m}$ , confirming the broad crystal size distribution in a ceramic material. Thus, we can conclude that the morphology of different black ceramic pigments depends mostly on other constituents ( $\text{Pb}_3\text{O}_4$ ,  $\text{SiO}_2$ ) but not

on the sol-gel-derived precursors  $\text{YFeO}_3$ ,  $\text{Y}_3\text{Fe}_5\text{O}_{12}$ ,  $\text{CoFe}_2\text{O}_4$ ,  $\text{ZnFe}_2\text{O}_4$  or  $\text{NiFe}_2\text{O}_4$ .

The prepared five different black pigments were placed on the oven-dried ceramic plates and annealed for 5 h at 800  $^\circ\text{C}$ . After annealing, novel black glazes based on the transition metal ferrites were synthesized. The SEM images of the ob-

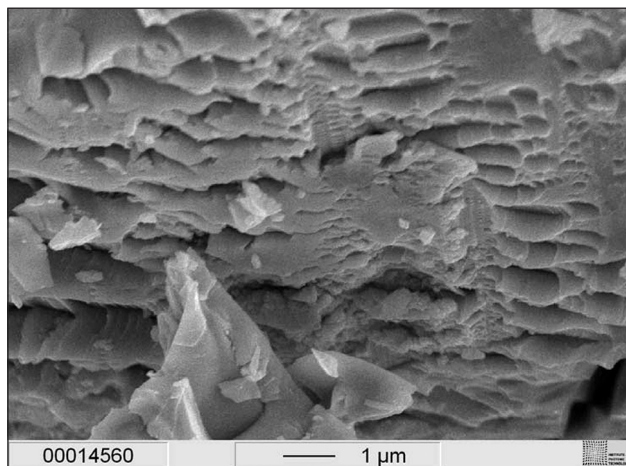


Fig. 8. SEM micrograph of  $\text{CoFe}_2\text{O}_4$ -based black pigment

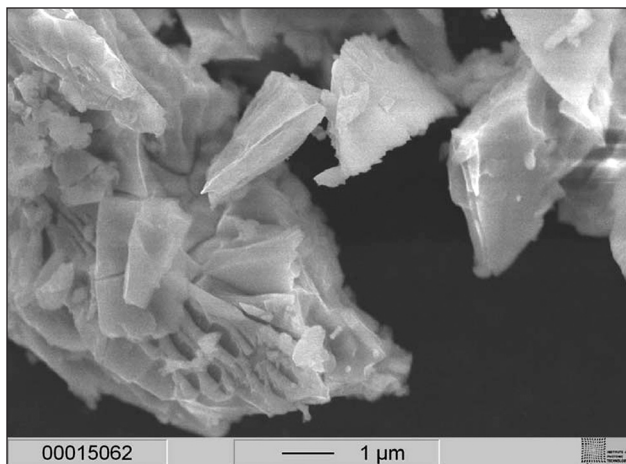


Fig. 9. SEM micrograph of  $\text{NiFe}_2\text{O}_4$ -based black pigment

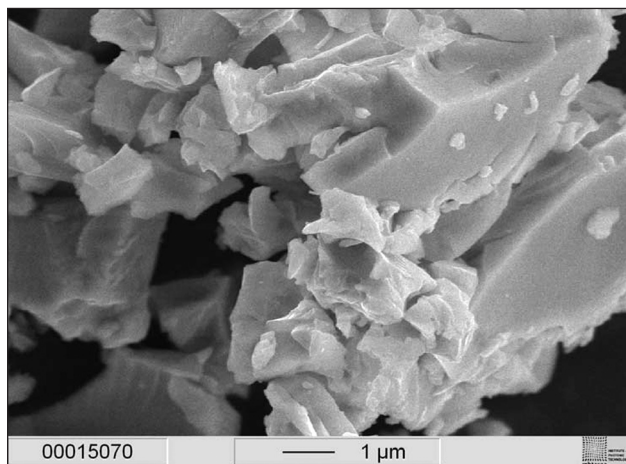


Fig. 10. SEM micrograph of  $\text{ZnFe}_2\text{O}_4$ -based black pigment

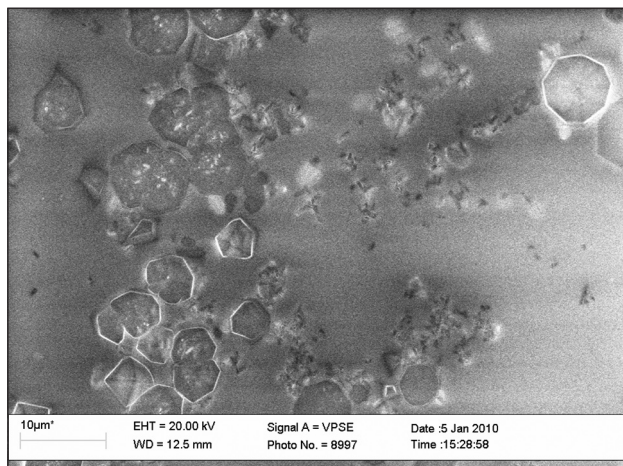


Fig. 11. SEM image of black glaze with  $\text{YFeO}_3$

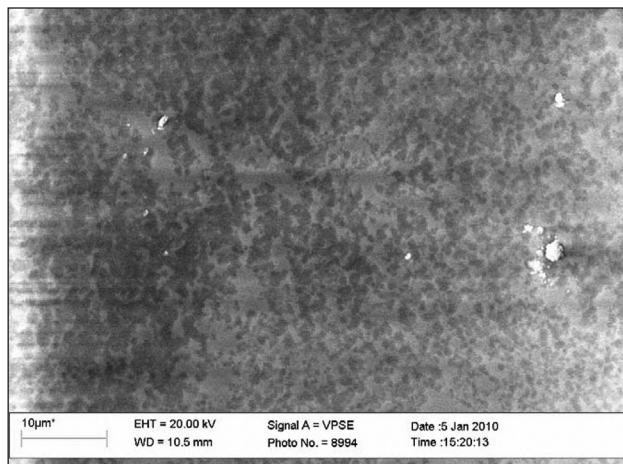


Fig. 12. SEM image of black glaze with  $\text{Y}_3\text{Fe}_5\text{O}_{12}$

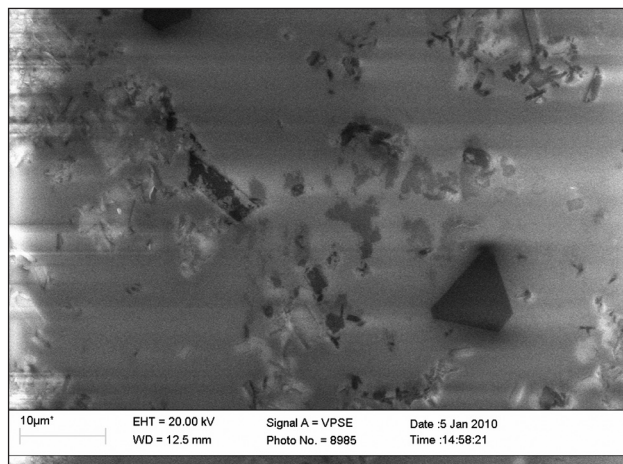


Fig. 13. SEM image of black glaze with  $\text{CoFe}_2\text{O}_4$

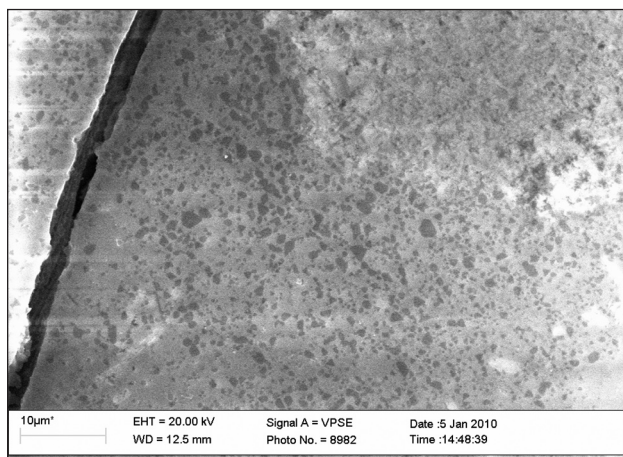


Fig. 14. SEM image of black glaze with  $\text{NiFe}_2\text{O}_4$

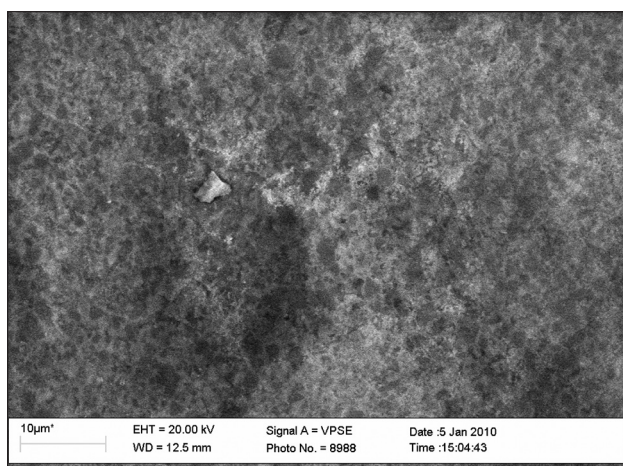


Fig. 15. SEM image of black glaze with  $\text{ZnFe}_2\text{O}_4$

tained black glazes are shown in Figs. 11–15. It is evident from SEM micrographs that the surface of glazes from the  $\text{YFeO}_3\text{--CuO}$  and  $\text{CoFe}_2\text{O}_4\text{--CuO}$  mixtures contains separate crystallites (Figs. 11 and 13, respectively). However, SEM micrographs of the other three samples (Figs. 12, 14 and 15) show a fine microstructure with a smooth surface of black glazes. In conclusion, for the preparation of new black glazes, nanoscaled transition metal ferrites synthesized using a simple environmentally benign sol-gel method could be suggested.

## CONCLUSIONS

In this work, for the synthesis of yttrium perovskite ferrite ( $\text{YFeO}_3$ ), yttrium iron garnet ( $\text{Y}_3\text{Fe}_5\text{O}_{12}$ ), cobalt, nickel and zinc iron spinels ( $\text{CoFe}_2\text{O}_4$ ,  $\text{NiFe}_2\text{O}_4$  and  $\text{ZnFe}_2\text{O}_4$ , respectively), an environmentally benign aqueous sol-gel process has been suggested. These transition metal nanoferrites were successfully used for the preparation of black ceramic pigments and glazes. The obtained transition metal ferrites, pigments and glazes were characterized by scanning electron microscopy (SEM). Scanning electron micrographs

indicated the formation of nanosized  $\text{YFeO}_3$  and  $\text{Y}_3\text{Fe}_5\text{O}_{12}$  crystallites  $\sim 200$  nm in width and  $\sim 1000$  nm in length. The particle size of transition metal spinels was found to be dependent on the nature of a transition metal ( $\text{CoFe}_2\text{O}_4 > \text{ZnFe}_2\text{O}_4 > \text{NiFe}_2\text{O}_4$ ). Moreover, all three spinels had a mesoporous structure. The morphology of different black ceramic pigments, however, depends mostly on other constituents ( $\text{Pb}_3\text{O}_4$ ,  $\text{SiO}_2$ ) but not on the sol-gel-derived transition metal ferrites. The surface of glazes with  $\text{YFeO}_3$  and  $\text{CoFe}_2\text{O}_4$  contained separate crystallites. However, SEM micrographs of the other three samples with  $\text{Y}_3\text{Fe}_5\text{O}_{12}$ ,  $\text{NiFe}_2\text{O}_4$  and  $\text{ZnFe}_2\text{O}_4$  showed a fine microstructure with a smooth surface of black glazes.

## ACKNOWLEDGEMENTS

The authors are thankful to Dr. Edita Garskaite and Dr. Vladimir Sivakov for SEM measurements and helpful discussions.

Received 03 September 2010

Accepted 21 September 2010

## References

1. X. Y. Wang, G. Q. Yang, Z. S. Zhang, L. M. Yan, *Dyes Pigm.*, **74**, 269 (2007).
2. A. K. M. A. Hossain, H. Tabata, T. Kawai, *J. Magn. Magn. Mater.*, **320**, 1157 (2008).
3. G. Costa, V. P. Della, M. J. Ribeiro, A. P. N. Oliveira, G. Monros, J. A. Labrincha, *Dyes Pigm.*, **77**, 137 (2008).
4. U. Ozgur, Y. Alivov, H. Morkoc, *J. Mater. Sci. Mater. Electr.*, **20**, 789 (2009).
5. D. H. Kim, H. D. Zeng, T. C. Ng, C. S. Brazel, *J. Magn. Magn. Mater.*, **321**, 3899 (2009).
6. B. Raveau, V. Caignaert, V. Pralong, A. Maignan, *Z. Anorg. Allg. Chem.*, **635**, 1869 (2009).
7. J. S. Ghodake, R. C. Kambale, S. V. Salvi, S. R. Sawant, S. S. Suryavanshi, *J. All. Comp.*, **486**, 830 (2009).
8. P. Lavela, J. L. Tirado, *J. Power Source*, **172**, 379 (2007).
9. A. Rittidech, N. Porkornwong, A. Suthapintu, *Ferroelectr.*, **382**, 62 (2009).
10. D. Li, Z. J. Peng, X. M. Cui, C. B. Wang, H. L. Ge, Z. Q. Fu, Y. Y. Yang, *Rare Met. Mater. Eng.*, **38**, 920 (2009).
11. W. W. Ling, H. W. Zhang, Y. He, Y. Wu, K. Yang, Y. X. Li, S. Li, *J. Magn. Magn. Mater.*, **322**, 819 (2010).
12. E. Garskaite, K. Gibson, A. Leleckaite, J. Glaser, D. Niznansky, A. Kareiva, H.-J. Meyer, *Chem. Phys.*, **323**, 204 (2006).
13. K. Sadhana, R. S. Shinde, S. R. Murthy, *Int. J. Modern Phys. B*, **23**, 3637 (2009).
14. X. Z. Guo, B. G. Ravi, P. S. Devi, J. C. Hanson, J. Margolies, R. J. Gambino, J. B. Parise, S. Sampath, *J. Magn. Mater.*, **295**, 145 (2005).
15. M. R. Barati, S. A. S. Ebrahimi, A. Badii, *J. Non-Cryst. Solids*, **354**, 5184 (2008).
16. M. Gharagozlu, *J. All. Comp.*, **486**, 660 (2009).

17. S. Yanez-Vilar, M. Sanchez-Andujar, C. Gomez-Aguirre, J. Mira, M. A. Senaris-Rodriguez, S. Castro-Garcia, *J. Solid State Chem.*, **182**, 2685 (2009).
18. A. L. Xia, H. L. Zhang, *Cur. Appl. Phys.*, **10**, 825 (2010).
19. J. Livage, M. Henry, C. Sanchez, *Progr. Solid State Chem.*, **18**, 259 (1988).
20. B. L. Cushing, V. L. Kolesnichenko, C. J. O'Connor, *Chem. Rev.*, **104**, 3893 (2004).
21. J. D. Mackenzie, E. P. Bescher, *Acc. Chem. Res.*, **40**, 810 (2007).
22. A. Katelnikovas, J. Barkauskas, F. Ivanauskas, A. Beganskienė, A. Kareiva, *J. Sol-Gel Sci. Techn.*, **41**, 193 (2007).

Aurelija Gatelytė, Jūratė Senvaitienė, Darius Jasaitis,  
Aldona Beganskienė, Aivaras Kareiva

### ZOLIŲ–GELIŲ METODU SUSINTETINTŲ PRADINIŲ MEDŽIAGŲ, NAUJŲ JUODŲJŲ PIGMENTŲ IR GLAZŪRŲ APIBŪDINIMAS SEM METODU

#### S a n t r a u k a

Vandeniniu zolių–gelių metodu susintetinti itrio perovskitinis feritas ( $\text{YFeO}_3$ ), itrio geležies granatas ( $\text{Y}_3\text{Fe}_5\text{O}_{12}$ ) ir kobalto, nikelio bei cinko špineliai ( $\text{CoFe}_2\text{O}_4$ ,  $\text{NiFe}_2\text{O}_4$  ir  $\text{ZnFe}_2\text{O}_4$ ). Šie feritai buvo sėkmingai panaudoti naujų keraminių juodųjų pigmentų bei glazūrų sintezei. Gautų junginių bei kompozicijų morfologija tirta skenuojančios elektroninės mikroskopijos (SEM) metodu. Nustatyta, kad susidarė nanoeilės  $\text{YFeO}_3$  ir  $\text{Y}_3\text{Fe}_5\text{O}_{12}$ , kurių kristalitų plotis buvo apie 200 nm, ilgis – apie 1000 nm. Pereinamųjų metalų špinelių kristalitų dydis nežymiai priklauso nuo metalo prigimties ( $\text{CoFe}_2\text{O}_4 > \text{ZnFe}_2\text{O}_4 > \text{NiFe}_2\text{O}_4$ ). Tačiau juodųjų pigmentų morfologinės savybės tiesiogiai nepriklauso nuo pereinamųjų metalų feritų, o priklauso nuo kitų pigmentų sudedamųjų dalių ( $\text{Pb}_3\text{O}_4$ ,  $\text{SiO}_2$ ). Be to, gautų juodųjų glazūrų su  $\text{YFeO}_3$  ir  $\text{CoFe}_2\text{O}_4$  paviršiuje nustatyti atskiri kristalitai. Naujos juodosios glazūros su  $\text{Y}_3\text{Fe}_5\text{O}_{12}$ ,  $\text{NiFe}_2\text{O}_4$  ir  $\text{ZnFe}_2\text{O}_4$  pasižymėjo lygiu paviršiumi ir reikiamomis morfologinėmis savybėmis.